Comparison of strain gage technique and photoelastic coating method in the investigation procedure of femur prostheses

Dr. Lajos **Borbás** Ph.D.
Budapest University of Technology and Economics, Department of Vehicle Parts and Drives

Dr. Frigyes **Thamm** Ph.D.
Budapest University of Technology and Economics, Department of Applied Mechanics

László **Oláh** mech. eng. student
Budapest University of Technology and Economics, Department of Polymer Engineering

1. INTRODUCTION.

There are numbers of *femur head prostheses* of different shapes used in *traumatological* surgery. The comparison of their efficiency is highly difficult due to the irregularities of the individual femur shape and the procedure of their "driving in" into the femur channel. Different positions during the movement of the person (walking, running, stepping on stairs etc.) cause more or less different stress distribution in the femur and especially along the contact surface between the femur channel and the stem of the prosthesis. Thus the obtaining of the suitable shape of the prosthesis became difficult and this resulted in different designs dependent on the opinion of the surgeon about the relative danger caused by one or another load position on the femur. The main differences between the particular parts of the prosthesis included the shape of the central line of the stem (straight or curved) and its cross section along its length (nearly circular or more or less lengthy). Additional problems arose from the scatter of the elastic and strength properties of the cortical and *trabecular* bone [1][2]. A number of theoretical investigations were carried out [3]-[8] which yielded some insight in the mechanism of force transfer between the prosthesis and the femur shaft but due to the necessary simplifications made during the calculations they could yield only guidelines for the recommended shape of the prosthesis.

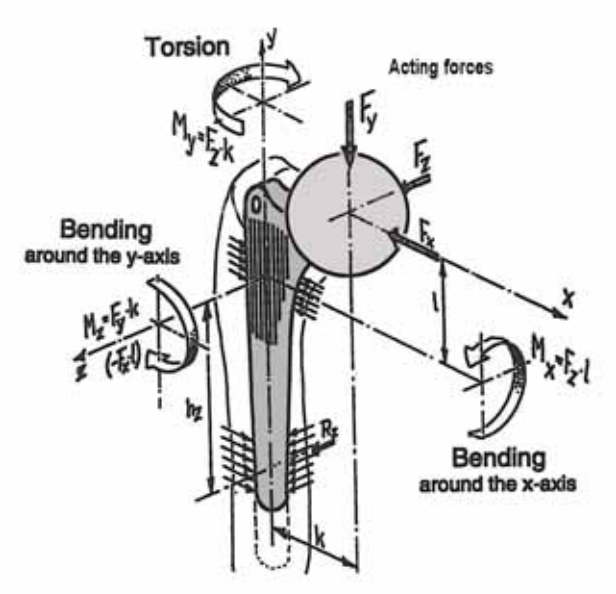

Fig.1.
The external forces and moments acting on a femur prosthesis.

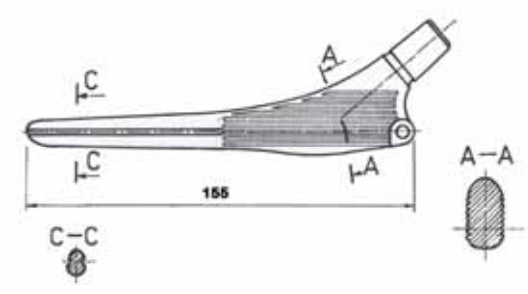

Fig.2.
Prosthesis type *MY*. The vertical grooves on the upper half of the stem were intended to withstand the torsion moment M_y as shown in *Fig. 1*.

In *Fig.1.* all possible components of the external forces and moments acting upon the prosthesis are collected. Most of them create normal contact stresses between the prosthesis stem and the femur shaft provided good ingrown bond between both. Force F_y and moment M_y have to be transmitted to the bone by interface shear. Especially the latter may cause failure especially for prostheses whose stem has an approximately circular cross section. Thorough optical mapping of a femur shaft actually revealed a cross section of such shape also [13], the result of it should be discussed in point 3. Axial ribbing of the prosthesis [9] or surface treatment of the prosthesis stem [10] may improve the contact but may also create failure of the stem.

Implant longevity depends on the stability of the prosthesis in the bone. Relative movement of the prosthesis against the bone must lie under a very low value [11] and the contact stress between both should also be as smooth as possible. To obtain the necessary experience of prosthesis design, experiments on cadavers have to be carried out. The problem is however, that measurements can be carried out mostly only at the outer surface of the femur, letting possible contact stress concentrations remaining hidden. Interpretation must depend therefore on the thorough evaluation of the stress patterns obtained in the experiments.

2. PRELIMINARY EXPERIMENTS

The joint cooperation between the Dept. *of Traumatologic Surgery of the St. Johns Hospital* in Budapest under the leadership of *Prof. G. Krakovits*, and the *PROTETIM Inc. for Medical Devices*, (led by the director *I. Juhász*) and the *KALIBER Műszer és Méréstechnika Inc*. (Enterprise for Mechanical Measurement led by the technical director *I. Ballon*), and the *Dept. of Applied Mechanics*, and the *Dept. of Vehicle Parts and Drives of the BUTE* resulted some preliminary work in the field of biomechanics applying different kinds of strain measurement technologies [14].

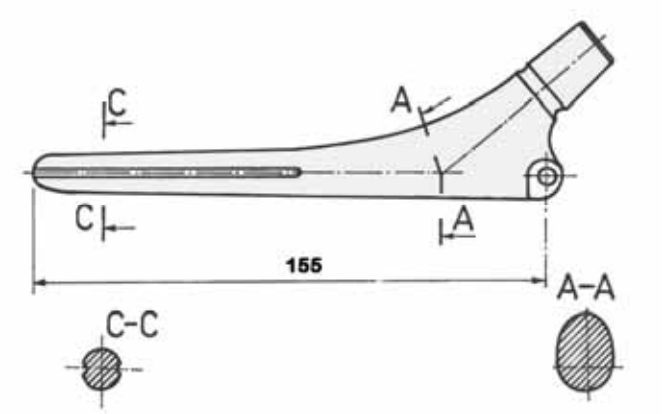

Fig. 3.
Prosthesis type *KR*

Fig. 4.
A femur with the indrawn prosthesis with bonded strain gages.

To obtain some insight into the influence of the shape of the prosthesis stem on the contact stress distribution two series of strain gage measurements were carried out by the authors provided with different prostheses made by the *PROTETIM Co*. and widely used in Hungary.
In the first series an intact bone (*No.1*) was compared with three femurs with prostheses as follows: *No.2*.: un-cemented prosthesis with narrow cross section *(Type "MY"), No.3*.: un-

cemented prosthesis with nearly circular cross section of the stem *(Type "KR"), No.4.*: Cemented prosthesis *(Type "KR")*. The notations follow those used by *PROTETIM*. The shape of the prostheses are shown in *Figs 2* and *3*.
Vertical load of $F_y = 425\ N$ was applied. One of the specimens with the strain gages bonded on it and placed into the loading rig is shown in *Fig.4.* The measured strains plotted over the femur length are collected in *Fig.5*. As the gages No. 56, 70 and 58 were in vertical position they indicated strain in this direction. Only gage No. 55 indicated the presence of hoop or shear stress but no clear conclusions could be drawn from it about the question which of the prostheses would be favourable.

In a second attempt *uniaxial* loading by the force F_y was compared with a combined load consisting of F_y and a torsion moment $M_t = a \cdot F_{xt}$ as seen in *Fig.6.* From the strains measured approximate stress values were calculated by multiplying them simply with estimated *Youngs moduli* based on data from [1]. As seen from the plot of the stresses the applied positions of the strain gages proved to be insensitive against possible shear stresses caused by the torque. Application of strain rosettes on more points of the bone surface would have been more effective, but the evaluation of multi-axial stress states would have been difficult because of the anisotropic elasticity of the bone material.

3. APPLICATION OF *PHOTOELASIC* COATING

As shown above, pointwise measurement is not sufficient in obtaining a sound impression about possible stress peaks whose location is not known. Therefore *photoelastic* coating technique was applied. The coating was about *2 mm* thick and consisted from a *flexibilized* epoxy resin in order to minimize its stiffening effect upon the femur as investigated by *Cristofolini* [12]. The strain-optical constant S_ε of the coat was determined in the usual way on a strip of it bonded on a cantilever beam loaded to known deflection.

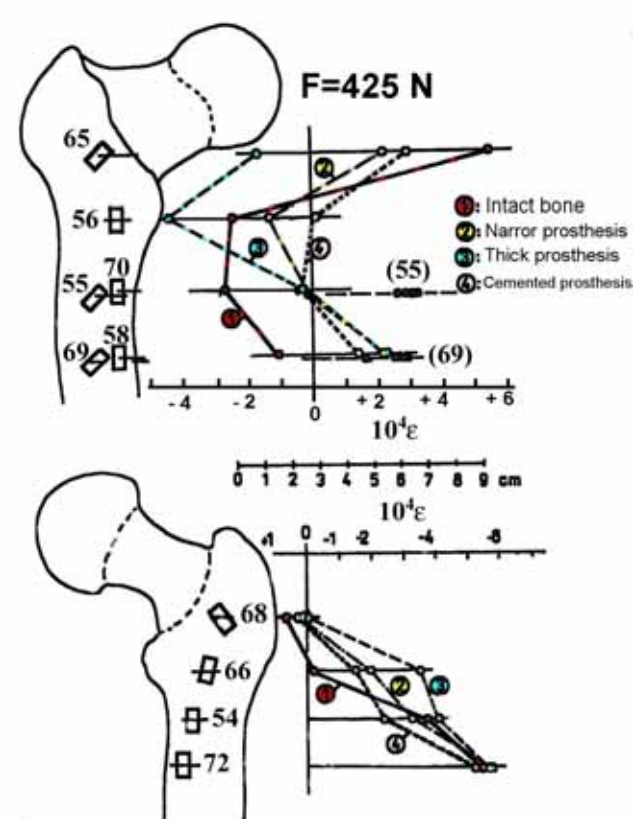

Fig.5.

Strain distribution on four different species evaluated from the strain gage data:
1.: Intact bone, 2.: prosthesis with narrow stem, 3.: Prosthesis with a thick stem, 4.: cemented prosthesis.

The actual value of the strain-optical constant was: S_ε= 1,04.10^{-3} strain/fringe order.

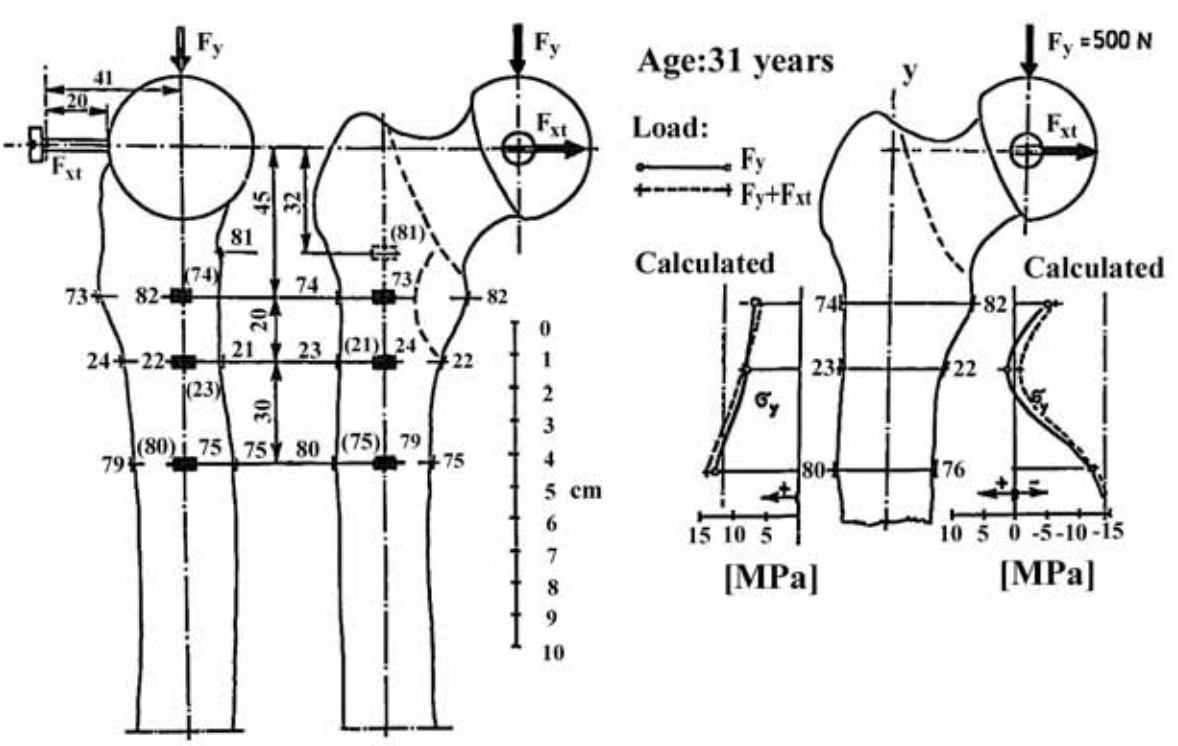

Fig.6.
The position of the strain gages and evaluated strain distribution from an experiment with two different loading mode
(bending, bending + torsion)

To obtain a pattern of the whole surface of the femur the investigated specimen together with the loading rig was mounted on a turntable. The full *isochromatic* fringe pattern was then combined from pictures taken by turning the loading rig in steps of 30^0.

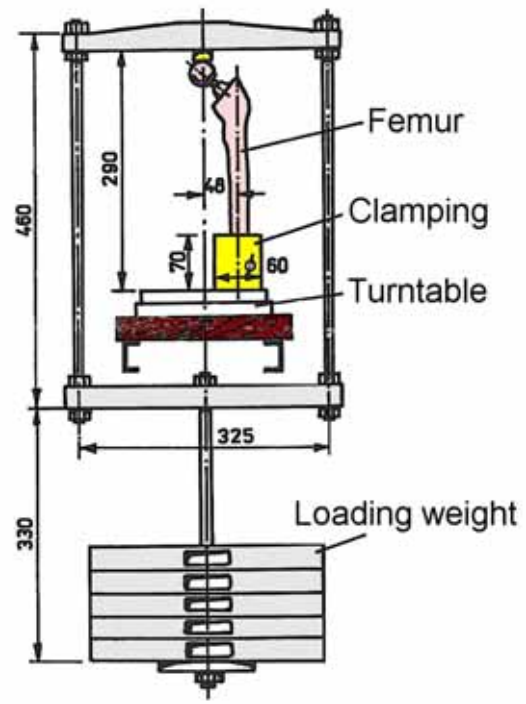

Fig.7.
The investigated femur in the loading rig

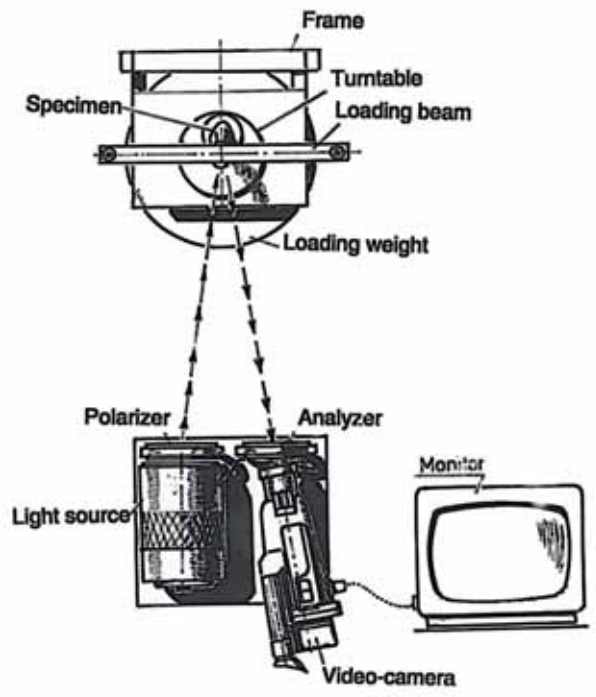

Fig.8.
The measuring set-up for the *photoeleastic* investigation

The side view of the assembly is shown in *Fig.7.,* and the complete instrumentation including the reflection *polariscope* provided with a video-camera and the attached monitor in *Fig.8.*

Patterns of six specimens were obtained, the data of which are collected in *Table I.*

Table. I.
The data of the specimens which underwent *photoelastic* investigation.

Number	Type of prosthesis *	Stem Shape	Fixation Method	Load *F [N]*	Load-free test	Axial compressive *Youngs* modulus ***E****[MPa]*
1	KR	Straight	Driving-in	735.5	Yes	$2.799.10^4$
2	KR	Straight	Driving-in		Yes	$1.306.10^4$
3	Mm	Curved	Bonding		No	$1.306.10^4$
4	Mm	Curved	Driving-in		Yes	$1.399.10^4$
5	MY	Straight	Bonding		No	$1.311.10^4$
6	- **	Intact Femur		612.9	No	$1.248.10^4$

* Notation of the *PROTETIM Co*.
** Not listed – origin unknown

To obtain patterns adjusting well to each other we had to depart from the standard ISO 7206 and positioned the axis of the femur shaft parallel to the rotational axis of the loading frame. To identify the position of the fringes a network of generators and contours of the cross sections were drawn on the specimens.
Their notations are collected in *Fig.9.* As the *photoelastic* coating was bonded on the surface of the femurs with already mounted prostheses the observed fringe pattern did not show the stress distribution caused by the driving-in process of them.
To obtain data about the about the latter the prosthesis was – where it was possible - extracted from the femur and underwent a second *photoelastic* investigation without the external load (see *Table I.*) .

The *isochromatic* fringe patterns were determined at crossed and parallel *polarizers* showing the integer and half orders respectively. In one case *polarizers* inclined at 45^0 to each other were also applied producing fringes of ¼ and ¾ order. *Fig.10.* shows one characteristic flattened fringe pattern with the fringe orders noted along the fringes.
From the fringe patterns the difference of the principal strains can be obtained by the equation:

$$\varepsilon_1 - \varepsilon_2 = S_\varepsilon . m \qquad (1)$$

with ε_1 and ε_2 the two principal strains, S_ε the strain fringe constant and m the fringe order.

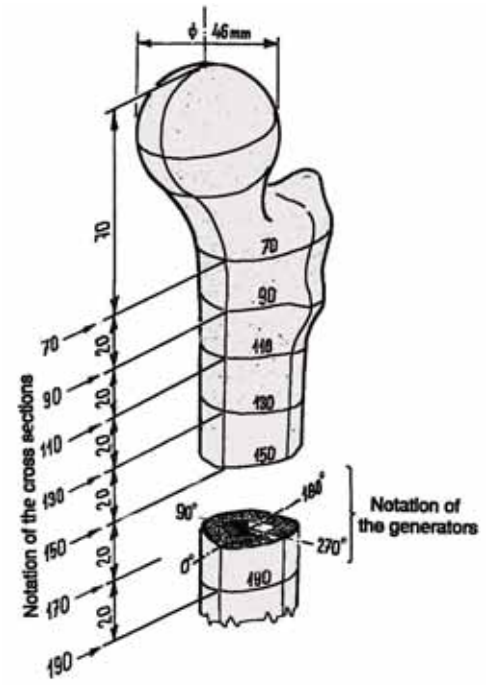

Fig.9.
The system of coordinate lines drawn upon the surface of the femur for the identification of the measurement results. 0^0: anterior, 180^0: posterior.

It should be noted, that the principal strain and principal stress difference is always positive. Regions of tension and compression can only be distinguished in case of pure *uniaxial* loading and compression which is assumed in the intact part of the femur shaft in case of loading as shown in *Fig.7.*

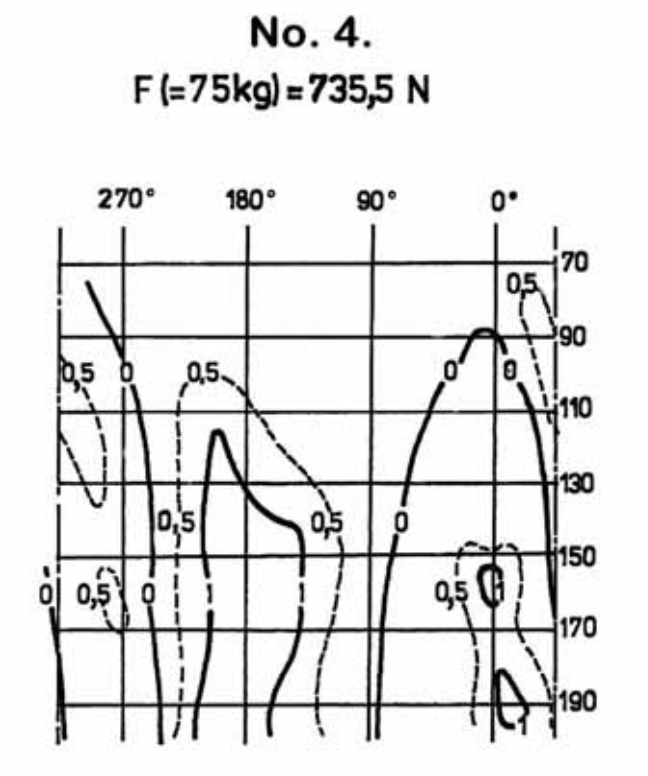

Fig.10.
Example of a flattened fringe pattern (specimen *No.4*. of *Table I.*). The notation of the cross sections and the generators correspond to that shown in *Fig.9.*

The sign of stress can be obtained applying the equilibrium conditions. Tension and compression is divided on the fringe patterns by a distinct line of zero fringe order.

To obtain stress values, the *Youngs* modulus and the *Poissons* ratio of the cortical bone is to be known. To avoid the necessity of using foreign data the fringe pattern of the lower part of the femur below the prosthesis stem was used as calibration specimen.

In an earlier work [13] the cross sectional data of femur shafts were calculated based on measurements of slices cut out of the shaft of the investigated femurs. A nearly circular shape with the principal axis of inertia lying approximately in the *x* and *z* direction as seen in *Fig.1.* was observed with the principal *moduli* of inertia being about $J_1 \approx J_z \approx 4{,}2.10^4$ mm^4 resp. $J_2 \approx J_x \approx 3.10^4$ mm^4 and the cross section area of about $A \approx 300$ mm^2 . In proper distance from the prosthesis stem tip only *uniaxial* stress state in the y-direction can be assumed resulting from the force F and the bending moment $F \cdot k$ (*Fig.11.).* The stress σ in a distance ξ from the centre of gravity of the cross section can be calculated according to elementary mechanics to:

$$\sigma = -F\left[\frac{k \cdot \xi}{J_z} + \frac{1}{A}\right] \tag{2}$$

the negative sign meaning compression. The highest value of it appears at point *P* of *Fig 9.* Considering the cross section of the femur shaft as cylindrical the negative stress peak will be

$$\sigma_0 = -F\left[\frac{k \cdot D}{2J_z} + \frac{1}{A}\right] . \tag{2a}$$

According to *Hookes* law the relation between the difference of the principal strains and stresses is – taking into account in *Eq.1*.:

$$\sigma_1 - \sigma_2 = \frac{E}{1+\upsilon}\left(\varepsilon_1 - \varepsilon_2\right) = \frac{E}{1+\upsilon} \cdot S_\varepsilon \cdot m = S_\sigma m \tag{3}$$

with S_σ the stress-fringe constant. Because of the uniaxial stress state σ_1 has to be zero, combining the fringe order $m = m_P$ at point *P* with *Eq. (2a)*

$$S_\sigma = \sigma_0 / m_P \tag{4}$$

is obtained, which allows the transition from fringe values to stresses. Assuming the *Poissons ratio* to $\nu = 0{,}4$, formulas (3) and (4) allow an estimation of the *Youngs* modulus also. Its values for the femurs investigated are therefore also collected in *Table.I.* Fair agreement with data found in [1] can be stated.

4. DISCUSSION OF THE RESULTS

According to *Eq.(2)* the external values of axial stress in the femur shaft have to appear at generators 0^0 (negative) and 180^0 (positive) of *Fig.9.* remaining approximately constant along the shaft length as long as its cross section does not alter nearing the femur head. This can be seen clearly in *Fig.12.* obtained from an intact femur (listed *No.6.* in *Table I.*) The figure also shows the stress distribution along the surface of the femur shaft at the cross sections 150 mm and 190 mm.

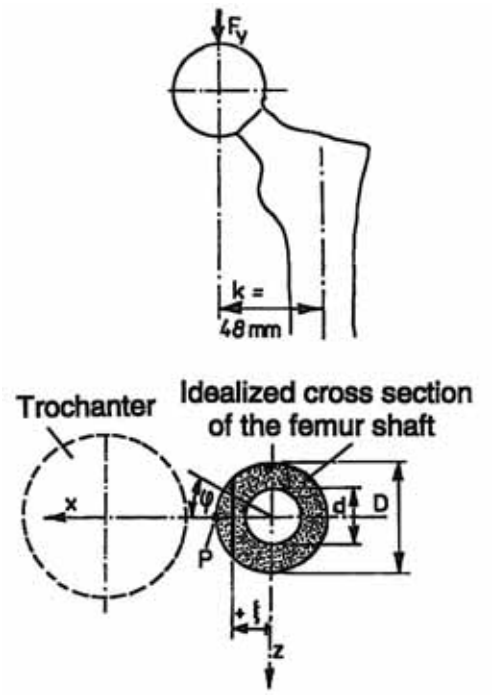

Fig.11.
The idealized cross section of the femur shaft on which the equations (2) and (2a) are based.

Fig.13. (*No.5*. in *Table I.*) shows a fringe pattern of a femur with bonded-in prosthesis. The similarity at the cross section l90 mm with that of *Fig.12.* indicates a perfect fit of the prosthesis in the femur channel.

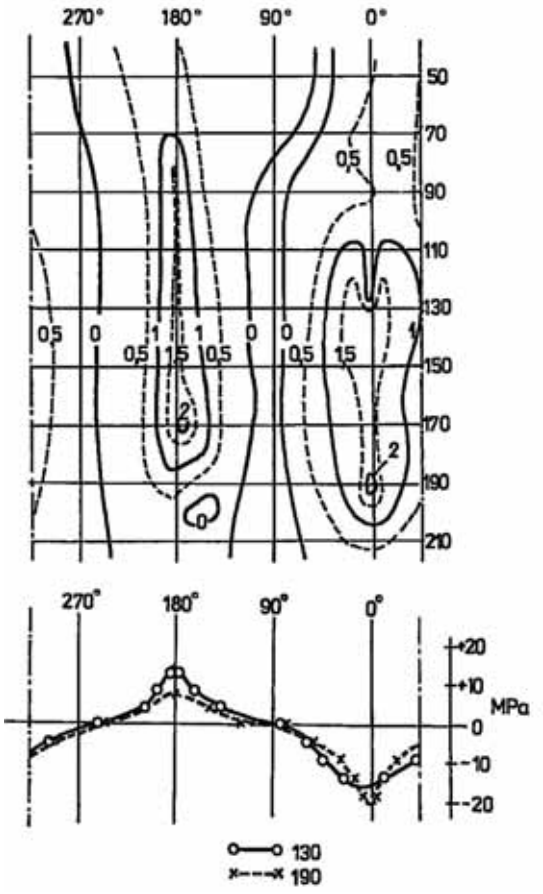

Fig.12.
The flattened fringe pattern of the intact femur *No. 6*. of *Table I.)* The lower part of the figure shows the (axial) stress distribution along two cross sections.

The drop of stress at higher cross sections (above 130 mm) is caused by the transition of the load from the femur shaft to the prosthesis stem as investigated in [7].

Figs 14. and 15. are flattened fringe patterns of the femur listed as *No.2.* in *Table I. Fig.14.* was obtained with the prosthesis driven in. Deviation of the loci of external stress values from the generator 0^0 (anterior) and that of 180^0 (posterior) especially at the plane 130 mm for tension and in the domain 200-250^0 for compression to 20^0 can be observed. From this it may be concluded, that the position of the prosthesis in the medullar channel is eccentric against the axis of symmetry of the femur shaft. The pattern taken after the extraction of the prosthesis (*Fig.15.)* shows traces of residual stress along the generators 90^0 and 270^0, which are remnants of plastic deformation having occurred during the driving-in procedure. Surely a less successful procedure than that of *No.5*. of *Table I.*

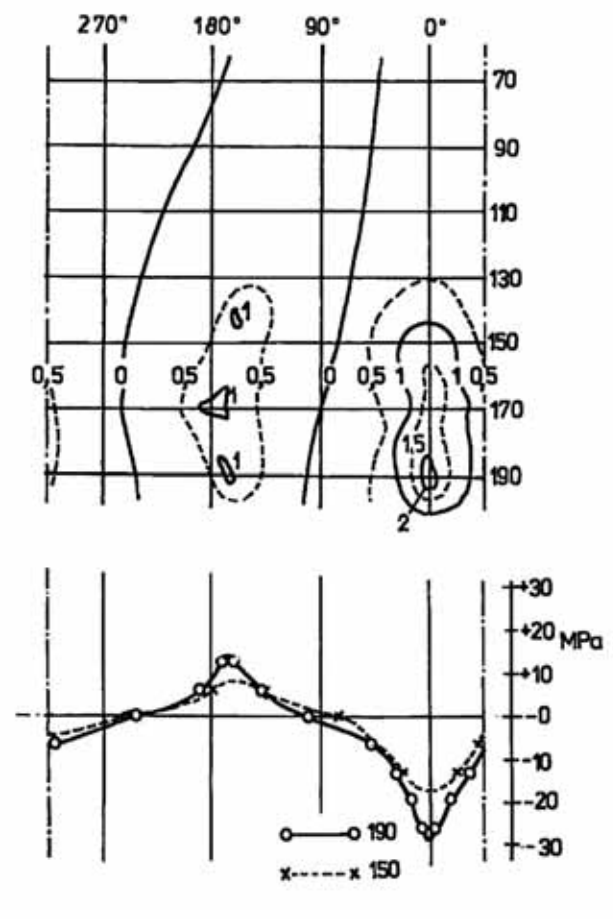

Fig.13.
The same as *Fig.10.* but taken from a femur with bonded-in prosthesis.(*No.5*.of *Table I.*)

The fringe pattern of the femur *No.4*.(*Fig.10.)* shows two local compressive stress peaks at 0^0 (anterior) between 150-190 mm. As the prosthesis applied had a curved stem, these peaks may be interpreted as the points of contact between the stem tip and the surface of the medullar channel.

To obtain more information the extraction of the prosthesis was carried out additionally and the pattern of the load-free femur was taken (*Fig.16.)* As seen from this, residual strain at the same region was found, justifying the assumption of overstraining the cortical bone at the points of contact, which may give cause for the degradation of the cortical bone and lead to the loosening of the prosthesis.

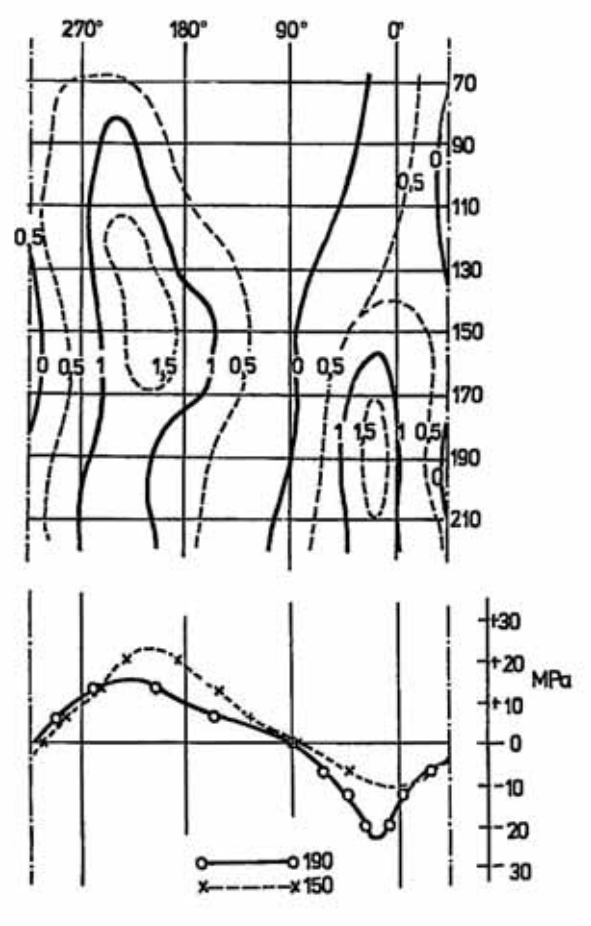

Fig. 14.
The same as *Fig.12.,* but taken from a femur with unbounded prosthesis (*No.2*.of *Table I.).* The stress pattern of the cross sections at 150 mm and 190 mm reveal a deviation of the external value from the generators 0^0 and 180^0. At the cross section of 130 mm the maximum is at $200\text{-}250^0$.

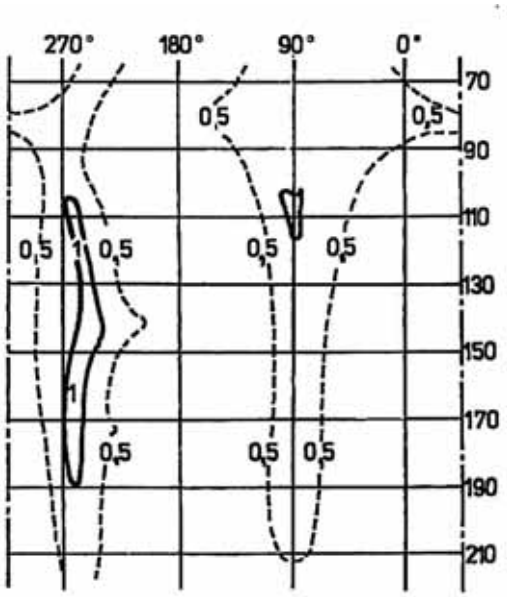

Fig.15.
Flattened fringe pattern of the specimen *No.2*. of *Table I.* unloaded after the extraction of the prosthesis. It is the pattern of the residual stress distribution caused by plastic deformation during the driving-in of the prosthesis.

The pattern of *Fig. 4.* represents a special case. The prosthesis has a stem of curved shape as shown in *Fig. 17.*
The two peaks at the generator of 0° indicate overstraining of the cortical bone at the stem tip. This justifies the opinion about the unfavourable behaviour of prostheses of such type as stated for instance by *Huiskes* [3].

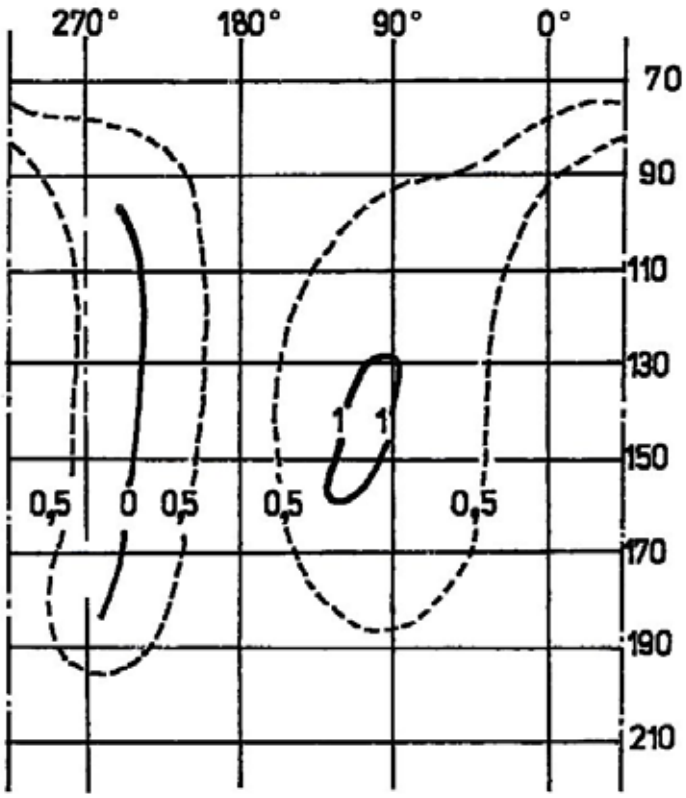

Fig.16.
The same as *Fig.15.,* taken from the Femur *No.4.* as shown earlier in *Fig.10.*

Fig. 17.
Prosthesis with curved central line (type Mm of Table I.) as applied in *Fig. 4.*

5. CONCLUSIONS

The examples shown reveal different individual stress distributions caused by minor deviations of the shape of the femur, different procedure of fixation and different shape of the prosthesis.
Though the stress peaks laying usually at the inner surface of the medullar channel and therefore they are directly not visible, the patterns may give good hints for surgical practice. To obtain more detailed information the continuation of such experiments would be advisable.

6. ACKNOWLEDGMENTS

The authors are indebted to the *PROTETIM Kft. (Orvostechnikai Üzem, Hódmezővásárhely)* for their support and to the *Kaliber Műszer és Méréstechnika Inc. (Budapest)* for giving auxiliary equipment to be disposal to carry out different biomechanical measurements.

The first international overview of the *photostress* measurement carried out by the authors applied on human bone materials was published in reference [14].

REFERENCES

1 Reilly, D.T. - Burstein, A.H.: The Mechanical Properties of Cortical Bone. Jr. of Bone and Joint Surgery .56 (1974) No.5. pp.: 1001-1022.
2 Lénárt, G. Tóth, I. - Pintér, J.: Experiments on the Hardness of Bone by Vickers Microhardness Measurements. Acta Biochimica et Biophysica Academiae Scientiarum Hungariae. 3 (1968) pp.: 205-215.
3 Huiskes, R.: Various Stress Patterns of Press-Fit, Ingrown and Cemented Femoral Stems. Clinnical Orthopaedics and Related Research Nr. 261(1990) pp.: 27-58.
4 Fethke, K. - Schmitz, K.P.- Plath, J.: Experimentelle und numerische Untersuchungen zur Verankerung von zementfreien Hüftenendprothesenmodellen. VDI-GMA-Bericht 29 (1996) pp.: 75-78.
5 Zacharias, Th. - Holzmüller - Laue, S.- Martin, H. - Schmitz, K-P. - Fethke, K. - Gerhardt, H.- Sungu, M.- Both, A.: Automatic Individual Finite-Element Analysis of Cement-less Hip-Implantations. Publication of the University of Rostock 1997.
6 Kirchner, I.: Emberi combcsont és protézis szilárdságtani vizsgálata. (Stress Analysis of Human Femur and Prosthesis) Ph.D. - Thesis. Budapest University for Technology and Economics. 1992.
7 Thamm, F.: Investigation of the Contact Stress Distribution Between the Femur Shaft and the Intermedullar Prosthesis. Proc. II. Congress on Mechanical Engineers (2000) Vol. I. pp.: 319-324. Budapest University for Technology and Economics
8 Pálfi, P.: A csontbiotechnika legújabb eredményei és azok alkalmazásai a combcsont numerikus vizsgálatában. (The Last Results of Biomechanics of the Bone and their Application in the Numerical Investigation of the Human Femur.) Lecture held at the IXth Hungarian Conference on Mechanics. Miskolc. 2003. To be published.
9 Beer, R.J. - Kodvanj, J. - Eberhardsteiner, J. - Grienauer, W. - Skrbensky, G. - Gottsauner, F.: Mechanical and optical Aspects of an Implant-Bone Connection in the Femur, Comparison of two solutions of Femur-Prostheses. Proc. of 16th Danubia-Adria-Symposium 1999. Cluj-Napoca pp.: 9-10.
10 Baleani, M.- Cristofolini, L. - Viceconti, M.: Investigation on Fatigue Limit of Hip Prostheses with Different Surface Treatment. Proc. of 13th. Danubia-Adria Symposium l996. Rajecke Teplice. pp.: 83-84.
11 Callaghan, J.J. - Fulghum, C.S. - Glisson, R.R. - Stranne, S.K.: The Effect of Femoral Stem

Geometry on Interface Motion in Un-cemented Porous-Coated Total Hip-Prostheses. Int. J. of Bone and Joint Surgery. 74-A (1992) No.6. pp.: 839-848.
12 Cristofolini, L.: Studio Fotoelastico su Femuri Umani con Protezi. Errori Sperimentali devuti al Rivestimento.
13 Thamm, F.: Determination of the Cross Sectional Data of a Cross Section of Irregular Shape. Proc. of 17th. Danubia-Adria Symposium, Prague. September, 2000. pp.: 321-323.
14 L. Borbás, F. - Thamm, - M. Hagymási, - G. Krakovits: Investigation of different design of femur head prosthesis with respect to the force transition to the femur shaft.
XXV AIAS International conference on material engineering. Gallipoli-Lecce, 4...7. September, 1996. p.: 245...248.

AFFILIATIONS

Dr. Lajos **Borbás** Ph.D., associate professor, Budapest University of Technology and Economics, Department of Vehicle Parts and Drives, Leader of the Central Research Laboratory of Biomechanical Research Center for Budapest University of Technology and Economics
borbas@kge.bme.hu, H-1111 Budapest, Bertalan L. u. 2. ☎ 463 1869, Fax: 463-1653

Dr. Frigyes **Thamm** Ph.D. associate professor, Budapest University of Technology and Economics, Department of Applied Mechanics, fthamm@mm.bme.hu

László **Oláh** Ph.D. Student, Budapest University of Technology and Economics, Department of Polymer Engineering, olah@pt.bme.hu